folia medica

Folia Medica 67(5)
DOI: 10.3897/folmed.67.e153885

Research Article

Optimizing CT imaging: a cutting-edge validation of quality assurance across scanners

Preethi Baskar[1], Sundaresan Sivapadham[2]

1 *Department of Radiodiagnosis, SRM Medical College Hospital & Research Centre, SRM IST, SRM Nagar, Kattankulathur, Chengalpattu (Dt), Tamil Nadu – 603203*

2 *Division of Medical Research, SRM Medical College Hospital & Research Centre, SRM IST, SRM Nagar, Kattankulathur, Chengalpattu (Dt), Tamil Nadu – 603203*

Corresponding author: Sundaresan Sivapatham, SRM University, Chengalpattu, Tamil Nadu, India; Email: preethib@srmist.edu.in

Received: 25 March 2025 ♦ **Accepted:** 1 June 2025 ♦ **Published:** 22 October 2025

Citation: Baskar P, Sivapadham S. Optimizing CT imaging: a cutting-edge validation of quality assurance across scanners. Folia Med (Plovdiv) 2025;67(5):e153885. doi: 10.3897/folmed.67.e153885.

Abstract

Introduction: A comprehensive test on a dual- and multi-slice CT scanner was carried out using in-house CT scanning with a CTDI phantom/test tool following the American Association of Physicists in Medicine's recommended methods to validate quality assurance of simulation CT and diagnostic CT.

Aim: To carry out the mechanical and radiation dose verification QA tests for the Siemens Emotion Duo CT simulator and GE CT as per the AERB QA protocol.

Materials and methods: The Siemens Emotion Duo is a twin-slice CT scanner that uses UFC dual-detector technology to provide sub-second scanning for a wide range of clinical applications. The precision-killed PMMA (polymethyl methacrylate) nested CTDI phantom has a 32 cm diameter body phantom and a 16 cm diameter head phantom. For the positioning of the PMMA for the CT ion chamber, the phantom is built with a central hole and either peripheral hole (four in the head phantom).

Results: Comprehensive QA and validation of results are necessary to obtain baseline data for CT virtual simulation and diagnostics. The results of QA data for CT equipment are compared and found to be within acceptable tolerance limits.

Conclusion: The results are unaffected by differences in collimations, reconstruction algorithms, or spectral energy because the data were collected over time on various CT scanners using the Piranha dosimetry.

Keywords

CT simulator, Siemens Somatom Emotion DUO, GE CT CTDI phantom, 0.1 cc ion chamber, Piranha 657

Introduction

A quality assurance program has the potential to contribute significantly to the production of images of consistently high quality with minimum patient exposure. This is achieved by aiding in the detection of changes in the image-producing variable and adversely affecting the quality of the image. Poor image quality can impede the accessibility of diagnostic information for medical professionals, thereby elevating the likelihood of an erroneous diagnosis. If a diagnosis is made on the basis of a poor image, the radiation exposure the patient has received will have been entirely superfluous. In the event that a radiography is repeated, the patient's exposure is naturally doubled. Data from the surveys suggest that some patients may be subjected to unnecessary radiation exposure on a regular basis. The extent of radiation exposure for a given patient can vary significantly between facilities, with some facilities reporting exposure levels that are 50 times higher than others. As with all imaging systems, the CT system necessitates the execution of quality assurance (QA) tests on a daily, monthly, and yearly basis.[1] Computed tomog-

Copyright by authors. This is an open access article distributed under the terms of the Creative Commons Attribution License (CC-BY 4.0), which permits unrestricted use, distribution, and reproduction in any medium, provided the original author and source are credited.

PENSOFT.

raphy (CT) scanning is a diagnostic imaging procedure that utilizes X-rays and advanced computerized technology to generate cross-sectional images of the body from multiple angles. The Piranha 657 model has been designed for utilization in a variety of applications, including CT, fluoroscopy, mammography, and radiography. The device is capable of measuring HVL, total filtration, time, dose/dose rate, and kVp. The same model dosimetry has been applied to diagnostic and simulation CT in four centers for quality assurance **(Table 1)**.

Several key scan parameters strongly influence CT image quality and the possibility of artifacts. Noise levels and tissue contrast are influenced by tube current (mA) and voltage (kVp), as slice depth and pitch affect spatial resolution and scan time, respectively. Higher mA and thicker slices reduce noise while increasing irradiance dose, but lower mA and thinner slices can lead to grainy images and motion distortion.[2] Incorrect choice of reconstruction algorithms and field of view can lead to loss of detail or aliasing. Furthermore, patient motion and incorrect positioning can lead to blurring and banding artifacts. As a result, careful adjustment of these parameters is necessary to ensure a high-quality image while reducing artifacts.

The American Association of Physicists in Medicine (AAPM) and Atomic Energy Regulatory Board (AERB) protocols were applied to examine four CT units from various models. These protocols included testing for accelerating voltage (kVp), mAs accuracy and its corresponding dose, half-value layer (HVL) measurement, machine output using a Piranha multimeter, and CTDI dose measurement using both head and body CTDI phantoms with 0.1 cc ion chambers.[3]

The CT scanner we used in the study employs the UFC dual detector technology to provide sub-second scanning for a wide range of clinical applications.[4] For excellent image reformatting, the Siemens Emotion Duo, a dual-slice CT scanner with UFC detector technology, offers anatomical volumes with thinner slices. In comparison to the single-slice scanners, it uses higher mA to enhance image quality and reduce X-ray tube load.[5] This spiral CT scanner has a 3.5 MHU tube, an 80-cm gantry aperture, and TFT rotation times of 0.8, 1, and 1.5 seconds. Slice thickness ranges from 1 to 8 mm, and gantry tilt ranges from –15° to +15°. Diagnostic CT scanners, except for gantry aperture and couch design, share similar specifications. The diagnostic CT gantry has a 68.58 cm diameter and a curved couch. The HPIPS CT scanner China has been using a sophisticated GE CT scanner device for picture collection. The GE CT scanner model has been analyzed using a convolutional neural network, which enhances the CT scanner's quality. It performs fast, low-dose scans without surrendering speed, power, or field of view.

Aim

The aim of the study was to assess whether the Piranha dosimeter approach is a reliable, sensitive, and acceptable QA test for AEC systems from four leading CT manufacturers. This test can be done in each different machine (i.e., A, B, C, D, and E).

The precision PMMA (polymethyl methacrylate) nested CTDI Phantom

The PMMA nested CTDI phantom, widely available in radiology departments, includes a central hole and four peripheral holes in the head phantom for CT ion chamber positioning. For CTDI measurements, the DTC10 is a tough, cylindrical, pencil-shaped air ionization chamber **(Fig. 1)**. The CT chamber is used to measure and track the output amount of exposure from CT scanners in a phantom or in an open environment. The IEC 61223-2-6 standard can be used to measure the CT dose index (CTDI). DTC10 can be connected to the Piranha to measure CTDI using a chamber adapter.[6] It is possible to link the DTC10 directly to the barracuda (using an electrometer module that supports bias measurement of the CTDI). The specifications of the 0.1 cc ionization chamber include a dose range of −0.8 mGy cm/s to 8 mGy cm/s, a length rate of Gy cm/s, an inaccuracy of ±6% or ±0.08 mGy cm, a 2 m low-noise triaxial cable, an active volume of 4.9 cm, an active length of 100 mm, an inner diameter of 8.0 cm, and typical leakage of ±4 fA.[7] Total filtration can be verified over a 100-meter Bluetooth range. QA experiments for the Siemens Emotion Duo and GE CT scanners followed the TG-66 protocol for both diagnostic and simulation CT.

Dosimetry – CTDI in air

A 10 cm pencil-shaped ionization chamber, positioned near the scan isocenter, quantifies the computed tomography

Table 1. Details of computer tomography scanners

Make	Slice	Model	Scan (t) (s)	Hospitals	Machine denoted as
Siemens	16	Somatom Emotion	0.6–1.5	GAACH & RC Kancheepuram Tamilnadu, India	A
Siemens	32	Somatom Spirit and 21109	0.8	SRM MCH & RC Kattangulathur Chennai, India	B
GE	32	REV ACTs Expert Edition	0.98	SRM Global Kattangulathur Chennai, India	E
GE	128	Optima CT660	0.675	SRM MCH & RC Chengalpattu, India	D

dose index (CTDI). A laboratory testing stand and a clamp support the ion chamber. The CTDI is expressed as[8]:

$$CTDI = 1/T \int_{-\infty}^{+\infty} D(Z)dz$$

where T is the nominal slice thickness, and D(z) is the dose profile along the tube's rotation axis. In helical mode, the CTDI is adjusted for overlapping slices by dividing by the pitch factor to calculate the multiple scan average dose (MSAD):

$$MSAD = CTDI / P$$

where pitch (P) is defined as r = Table Feed Per Rotation divided by Nominal Slice Thickness. The CTDI phantom is centered and aligned at the scan isocenter on the patient table. The ion chamber is inserted to measure the central CTDI, and peripheral CTDI is measured at least four times around the phantom to calculate an average.

Results

Laser QA procedure

The laser QA device is attached to the simulator tabletop, and the couch is adjusted until the side holes in the pegs align with the horizontal and vertical wall lasers.[8] Then both left and right wall lasers are verified to align with the holes within a tolerance of ±2 mm.

Scanner table test

The laser QA tool is placed as close as possible to the head of the tabletop (gantry side) and aligned with the gantry laser to capture a single image. The device is then moved as close as possible to the table's base and realigned with the gantry laser once more to capture a single image.[9] Two photos should be taken from the same position for the laser QA device. The center hole in the QA device is located using the scanner cursor tool on both images. The location of the hole should be within 2 mm of the location shown in both photos.

Gantry tilt

A square plastic sheet with water-equivalent properties is affixed to the pre-packed X-ray film and positioned with the sagittal gantry laser intersecting the film's vertical axis. A single scan is acquired at a 0° gantry angle with the narrowest slice thickness. The gantry is then tilted in both directions, and single scans are acquired at each position, near the limit of gantry movement.[10] The angle between the vertical and tilted exposures, measured with a protractor, should agree within ±1° of the digitally indicated gantry angle.[11] Resulting images show anterior-posterior (AP) and lateral (LAT) diameters. **Fig. 2** shows gantry angles that vary from 0° to 15°. At 0°, the AP and LAT diameters are equal. Gantry angle results for different machines (0.2°, 0.4°, 0.5°) are listed in **Table 2**.

Low contrast resolution

The smallest discernible item at a specific contrast level for a given dose is often referred to as low contrast resolution (or low contrast detectability) (LCR). The measurement is imperative to confirm during acceptance testing since it directly corresponds to imaging performance. LCR is assessed by imaging a low-contrast insert in at least 20 images and reviewed by at least three observers under ideal conditions to generate an average.[12] The LCR assessment by human observers demonstrated an overall increase in the mean reader score (better LCR) with increasing dose. However, in this study, the same dose value was set as 100 mA

Figure 1. Centre and peripheral CTDI calculated phantom setup.

Folia Medica

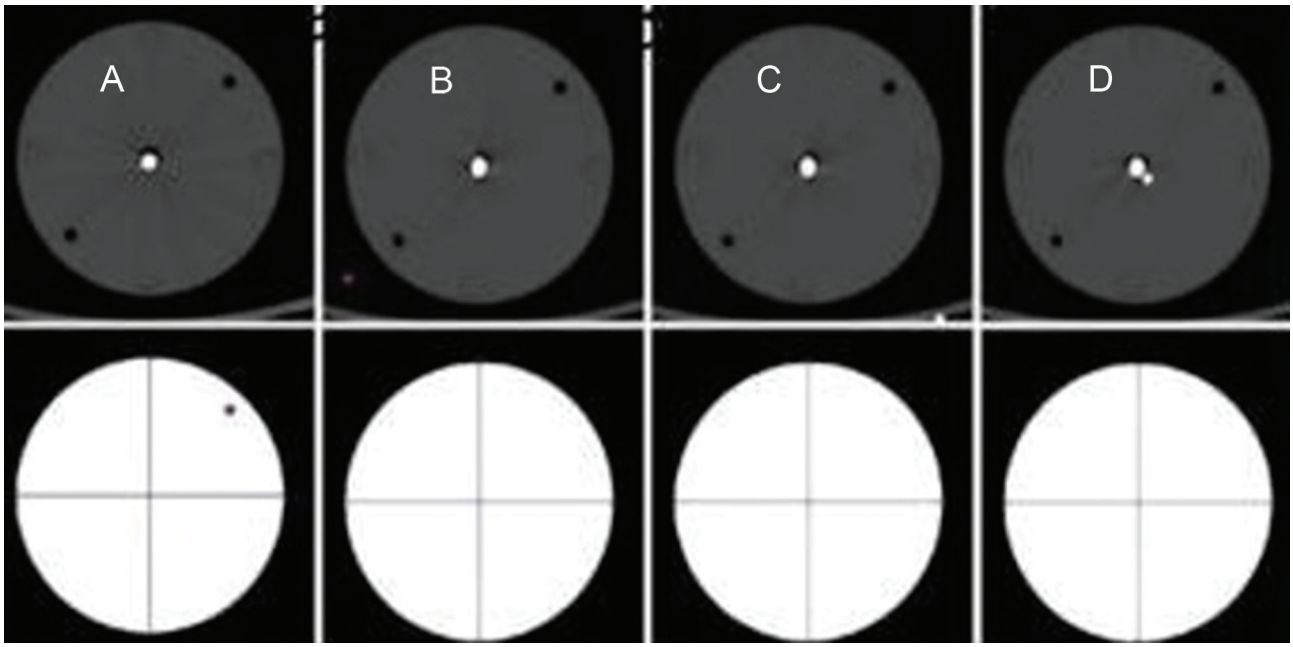

Figure 2. Gantry tilt test for A, B, C, and D.

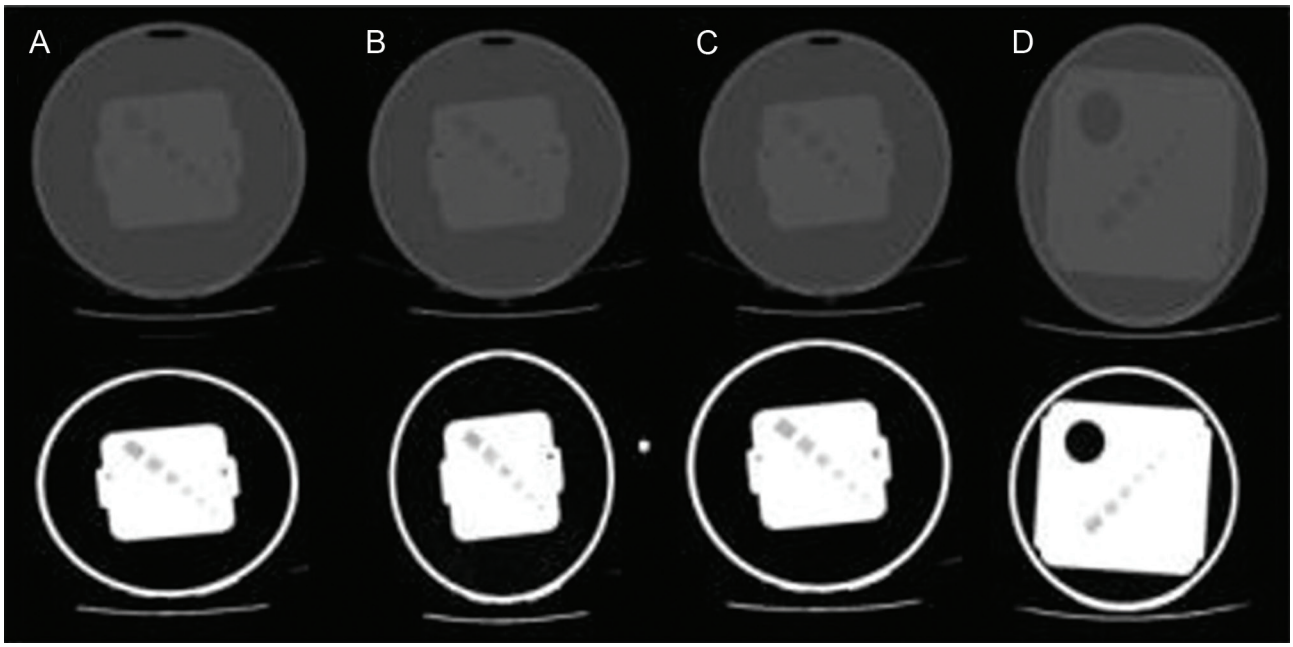

Figure 3. Low and high contrast test for A, B, C, and D.

and 120 kV. For vendors A, B, C, and D **(Fig. 3)**, the Picture Postcard Resolutions (PPR) for human observer assessment of the images' LCR were 10% (4.0), 8.3% (3.2), 8% (3), and 12% (5), respectively. Vendor D exhibited suboptimal contrast, yet its performance remained within the acceptable range of <15%, as defined by the established criteria.

The following report presents a summary of the mechanical safety performance test results for Somatom Siemens Medical CT and GE scanners.[13] The measured slice thickness accuracy of the CT scanner is tabulated, and the percentage of variation is shown to be within the tolerance limits at all kVp at 5 mAs for CT, as illustrated in **Table 2**. The measured operating potential for 80, 110, and 130 kVp was tabulated, and the variation was within the tolerance limit provided.

High contrast resolution

Two major categories of measuring techniques exist: the examination of the point spread function, typically through the determination of the modulation transfer function (MTF). The resolution is expressed as the spatial frequency

Table 2. A comparison of different CT dose quality and quantity factors (A, B, C, and D)

Type of machine denoted as	Accuracy of gantry tilt (degree)	Accuracy of slice thickness (mm)	Accuracy of operation potential (kV)	Timer accuracy (s)	Reproducibility of output (CoV)	Low contrast resolution (lp/mm)	High contrast resolution (lp/cm)	CTDI Centre peripheral (mGy)	CT Number accuracy (5HU)	Total filtration (mmAl)	Radiation leakage) (mR in hour)
Siemens 32 (A)	+15°	0.625	80	1.00	80			120 kV, 100 mA			
	−15°	1.000	110	1.50	110						
		4.000	130	2.00	120						
		5.000									
	0.2°	1.12	78.33	1.04	0.0015			Head 15.54	+6		
		3.80	109.6	1.52	0.0016	4.00	6.02	Body 7.26	−2	4.86	0.080
		4.90	128.3	2.02	0.0010						
Siemens 16 (B)	+15°	02.0	80	1.00	80			120 kV, 100 mA			
	−15°	05.0	100	1.50	100						
		10.0	120	2.00	120						
	0.4°	02.47	80.51	0.30	0.0003			Head 14.94	+7		
		05.05	99.41	0.30	0.0021	3.00	6.20	Body 8.55	−3	7.70	0.48
		10.02	119.60	0.30	0.0018						
GE 32 (C)	+15°	1.00	80	1.50	80			120 kV, 100 mA			
	−15°	3.00	100	1.00	100						
		5.00	120	0.50	120						
	0.5°	1.30	79.78	0.4%	0.0023			Body 5.29	+8		
		3.10	98.34	0.4%	0.0020	3.00	6.50	Head 15.456	−1	6.90	0.006
		5.20	119.7	1.3%	0.0010						
GE 128 (D)	+15°	2.00	80	1.0	80			120 kV, 100 mA			
	−15	3.00	130	1.5	120						
		5.00		2.0	130						
	0.3°	2.08	79.87	0.35%	0.005			Head 25.48	+6		
		2.96	131.7	0.35%	0.002	5.00	8.40	Body 13.71	−5	8.50	0.023
		4.44		0.35%	0.001						

(in line pairs per centimeter) at which the modulation falls to 50%, 10%, or 2% MTF, depending on whether it is determined through objective analysis or visual evaluation of images of a resolution bar phantom. The use of a body and head phantom facilitates the confirmation of slice thickness.[14] The stationary mode option in the service mode is employed to fix the exposure factors at a zero-degree angle. The phantom is positioned centrally on the table and exposed using a low kVp of 80 mAs and 2 mAs at intervals of 10 cm.

kVp accuracy

kVp accuracy is tested across the typical range (80, 110, and 130 kVp) at 100, 200, and 300 mA stations in localization scan mode with the tube above the table. Scans start 10 cm from one side of the detector and end 10 cm from the gantry, ensuring simultaneous irradiation. The kVp tolerance is ±2 kVp. Measured operating potentials for 80, 110, and 130 kVp are tabulated, with variations within the tolerance limit **(Table 2)**. The percentage deviation across four CT

Folia Medica

scanners is 8%, 7.3%, 7.8%, and 5%, respectively, within the ±10% tolerance.

The timer accuracy

The loading time must not deviate from the selected value by more than 10% +1 msec. Timer accuracy for exposure times of 1.0, 1.5, and 2.0 seconds across four CT scanners showed errors of 0.8%, 0.4%, 0.6%, and 0.75%, respectively, within acceptable limits.[15]

mR/mAs linearity

The mR/mAs linearity is verified at 110 kVp for a 1.0-second exposure at 100, 150, and 200 mA stations using the Piranha. The coefficient of linearity (COL) is calculated as:

$$\text{Coefficient of linearity (COL)} = \frac{X_{max} - X_{min}}{X_{max} + X_{min}}$$

The X-ray tube current must not deviate by more than 10% +0.2 mAs.

Output consistency

Output consistency is verified at 80, 110, and 130 kVp with 100 mAs and a 1-second exposure using the Piranha. The coefficient of variation (COV) is calculated as:

$$COV=X\text{-}1\ (å[Xi\ -X]2/n\text{-}1)½$$

*Tolerance in COV: ≤0.05

All COV values are below the tolerance of ≤0.05 for all CTs.

Total filtration

Total filtration is measured using the Piranha 657 at 110 kVp, 50 mA, and a 1-second exposure. For machine A, total filtration was 7.2 mm Al at 130 kVp, 100 mA, with a half-value layer (HVL) of 6.96 mm Al. For machine B, it was 5.78 mm Al at 110 kVp, 100 mAs, with an HVL of 4.86 mm Al. Tolerance for total filtration was 2 mm Al at 100 kV and 2.5 mm Al for machines A, B, C, and D, all within limits. The percentage variations between two CTs were −3.4%, −18.9%, −7.4%, and 8.4%, respectively.[16]

CT number accuracy

The reconstruction algorithm is responsible for generating the CT number, which is associated with the attenuation coefficient. The CT number range is from −1000 for air to +1000 for bone, with the value for water set at 0. Numbers that have been normalized in this manner are referred to as Hounsfield Units (HU).[17]

$$HU = \frac{\mu_m - \mu_w}{\mu_w} \times 1000$$

where μ_m is the material's attenuation coefficient and μ_w is the attenuation coefficient of water.

The CT number accuracy for water is verified using a water phantom filled with distilled water.[18] The water phantom is scanned at 130 kVp, 5 mm slice thickness, 50 mA, and a scan time of 68.29 seconds. The solid water phantom (30×30×30 cm^3) is positioned on the couch, and readings are recorded at various positions.[19]

The CT number accuracy test for water was carried out on four machines, and the results were tabulated. The tolerance level was ±5 HU, with a maximum of +6 HU and a minimum of −2 HU, all values being within the tolerance level.

CTDI measurement

The measurements of central and peripheral CTDI using a pencil beam ion chamber in head and body phantoms are shown in **Table 2**. The percentage of variation was within the tolerance limit for all CTs. Weighted CTDI (CTDIw) is equal to 1/3 $CTDI_{central}$ + 2/3 $CTDI_{peripheral}$. Stated CTDIW (head phantom): 6.55 mGy at 100 mAs, CTDIW (head phantom): 2.66 mGy at 100 mAs, measured CTDIW (head phantom): 8.661 mGy at 100 mAs, CTDIW (head phantom): 3.635 mGy at 100 mAs.

Radiation protection survey of CT

Radiation leakage from the X-ray tube casing at 1 meter (simulation CT and three diagnostic CTs) was measured at 130 kVp, 1 mAs, and 15 seconds. Leakage levels were 54 mR/hr (front cathode), 23.1 mR/hr (back anode), 1.14 mR/hr (left), and 1.94 mR/hr (right). Maximum leakage for a 500 mA/min workload was 4.5 mR/hr, below the recommended limit of ≤115 mR/hr. For a 180 mA/min workload at 110 kVp, 100 mA, and 1 second, leakage levels were 9.70 mR/hr (front cathode), 6.24 mR/hr (back anode), 2.31 mR/hr (left), and 6.12 mR/hr (right), with a maximum of 0.808 mR/hr, within limits.

Operating potential

kVp 110 kV, 100 mA, exposure time 1 second, workload 180 mA min/hr. At a distance of one meter from the machine, the measured radiation leakage was 9.70 mR/hr for the cathode, 6.24 mR/hr for the anode, 2.31 mR/hr for the left side, and 6.12 mR/hr for the right side.

kVp 130 kV, 500 mA, slice thickness 5 mm, exposure time 1 second. High leakage = 500 mA min in one hour × 9.70 mR/hr. The high leakage 60×100 mA was used for measurement.

As a result, we found that the highest radiation leakage at 1 meter from the casing for a workload of 180 mA min in an hour was 0.808 mR. The recommended upper limit leakage radiation level at 1 meter from the focus should be ≤115 mR in one hour.

Table 3. The radiation protection of computed tomography installation (Simulation CT)

S. No	Location	Survey meter reading µsv/hr
1	Lead lined door	1.07
2	Lead glass viewing window	
	A	2.96
	B	2.80
	C	3.10
3	Control console	
	A	0.08
	B	0.08
	C	0.17
4	Main entrance door	0.37
5	Linac server room	0.10
6	TPS room	0.10
7	Patient waiting area	0.05
8	Open space and road	0.08

Radiation protection of computed tomography installation (B, C, D)

Detail of radiation protection survey with mA: 100 kV: 110 and exposure time: 1.0. The maximum radiation level/week (mR/wk) = 150 mA min/week was 0.8, the high radiation level/week (mR/wk) was 0.02, and the permissible limit of radiation for a radiation worker was 20 mSv/year (40 mR/week) and for a member of the public was 1 mSv/year (2 mR/week). The radiation protection survey reading of the computed tomography installation was analyzed, and the percentage of variations was within the tolerance limits mentioned in **Table 2**.

Diagnostic practical cases and real patient and dynamic investigations.

A considerable number of artifacts from the early days of CT have been significantly reduced, yet some have persisted. The advent of new technologies has led to the emergence of more fully characterized artifacts, as Quality Assurance (QA) procedures are not conducted on an annual basis. **Figs 4, 5**, and **6** show some of the examples where artifacts were found in our department prior to QA.

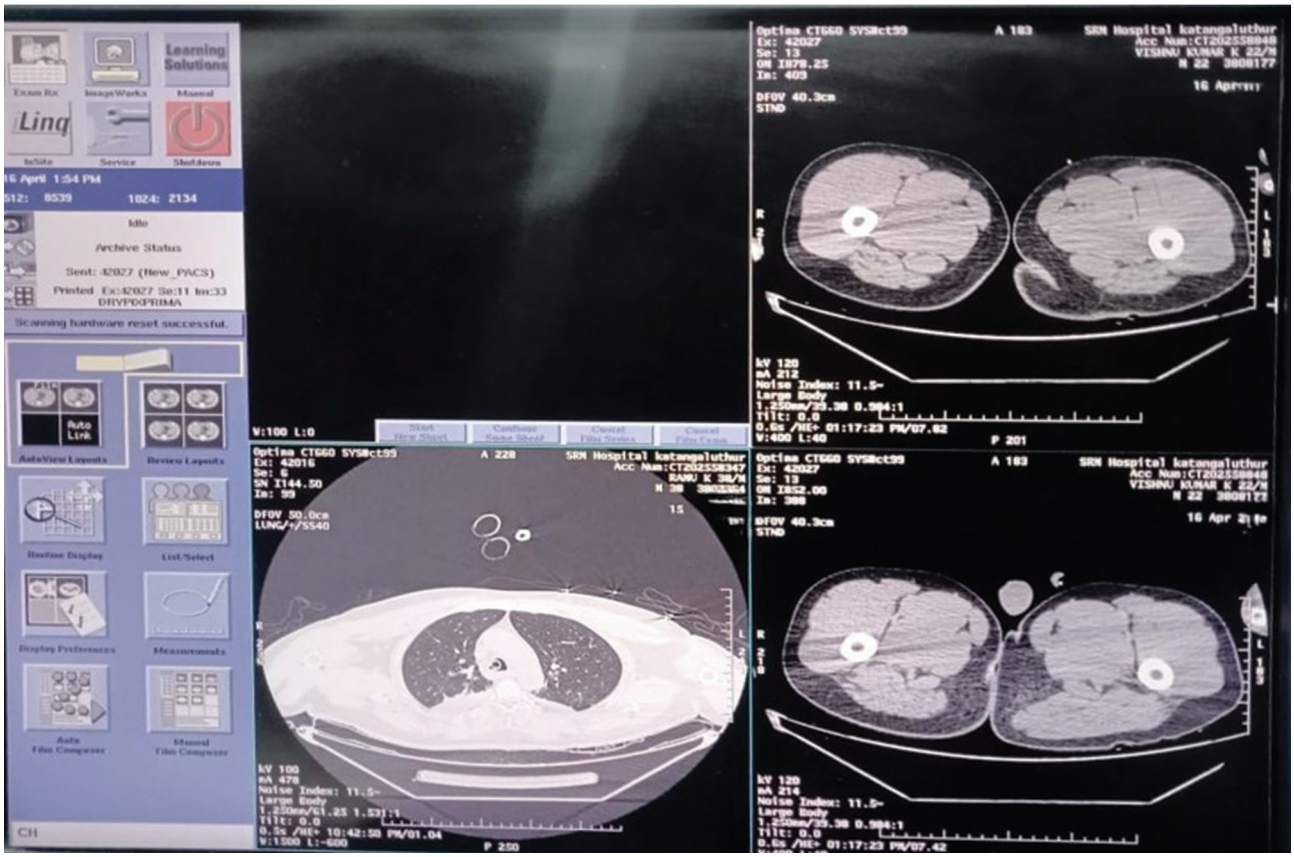

Figure 4. Artifact detected thorax images due to circular high-density areas in both thighs indicate metallic implants, likely orthopedic hardware. Surrounding them are dark streaks, typical of beam hardening and metal-induced streak artifacts surround them.

Folia Medica

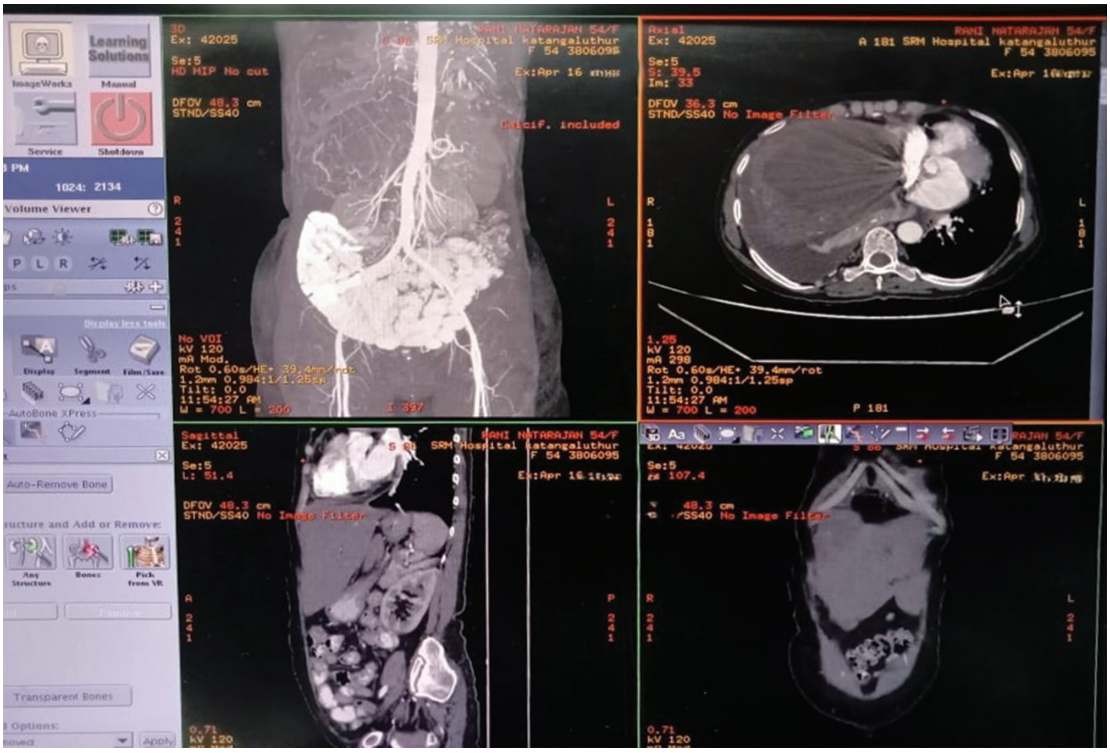

Figure 5. Streak artifact detected abdomen images due to CT contrast artifacts are image distortions caused by contrast media, appearing as streaks, blurring, or false enhancement. They can affect diagnosis but are reduced with proper timing, technique, and corrections.

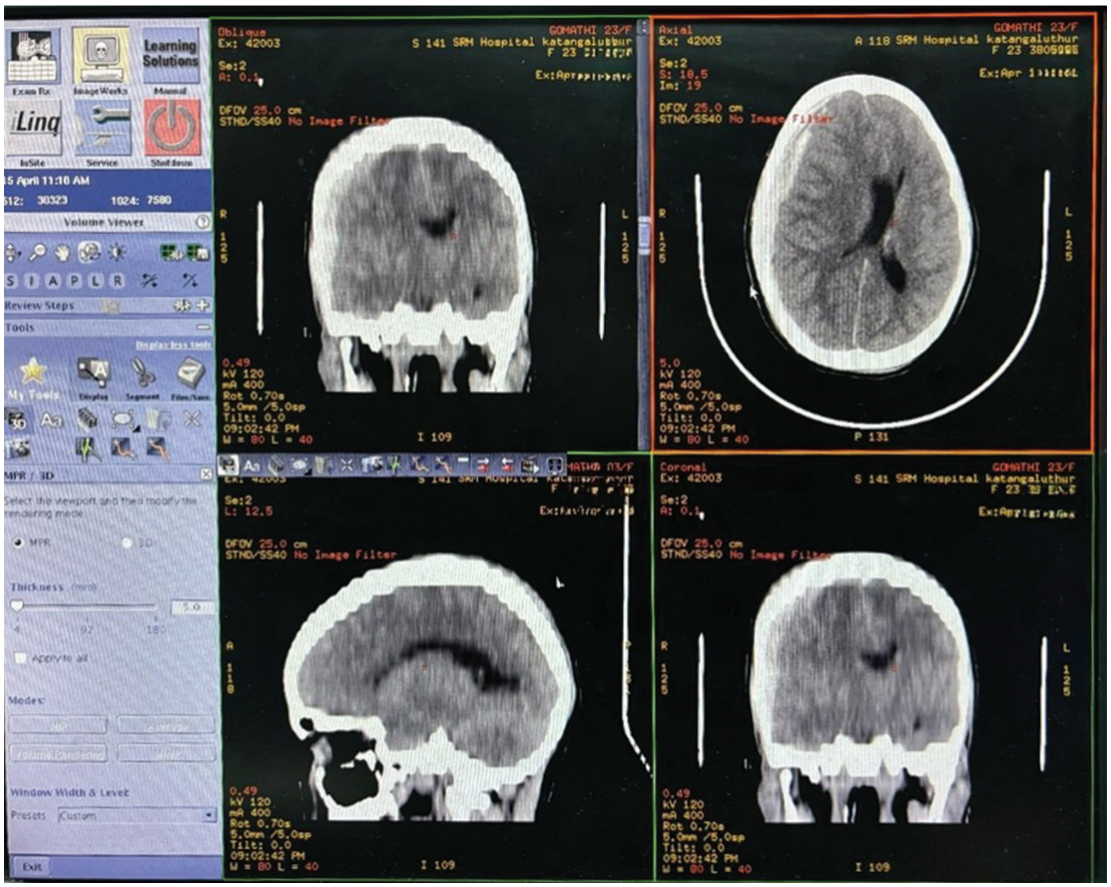

Figure 6. Streak artifact detected in brain images due to radiation dosage factor (also known as beam hardening artifact), most notably in the posterior fossa and periventricular area in some coronal and sagittal views. Electronic noise detected on impact with image noise.

Discussion

A series of mechanical and radiation tests for CT simulators and diagnostic CT have been conducted in accordance with the AERB protocol, and the results were found to be within the acceptable limits. The maximum deviation between the set slice thickness and measured slice thickness for different slice thicknesses of 1.4 mm and 5 mm was −0.2 mm. The maximum deviation between the set and measured kVp for 80, 110, and 130 kVp for different mA stations of 100, 150, and 200 mA was −17 kVp. The maximum percentage of timer error was 0.8% for 1.0 second. The same value has been repeated in the diagnostic CT.

The three parts address patient exposure: radiographic positioning, loading parameters, and entrance-skin exposure. The guidelines in each section are intended to improve the diagnostic quality of radiographs while reducing patient exposure. To minimize patient exposure, the set time and measurement time should be the same. Exposure is critical for timer accuracy tests since it can prevent overexposure to the subject.

The coefficient of linearity for 100, 150, and 200 mA stations was 0.0014, which is much less than the tolerance value of 0.1. The coefficient of variation of X-ray output consistency for 80, 110, and 130 kVp was 0.0013, 0.0005, and 0.0011, respectively. Values were much less than the tolerance value of 0.05. The total filtration for 110 kVp was well within the tolerance limit of 7.2 mm of Al equivalent.

The CTDI values displayed in the console for the head and body phantom match well with the measured CTDI, and they are well within the acceptable maximum tolerance limit of ±40% of the stated values, and the same result has been repeated for diagnostic CT.[20]

The resolution for high-contrast resolution images is 0.5 lp/mm, but the low-contrast resolution image resolved a 3 mm line pair at 1% contrast difference. The maximum leakage level of X-ray tube housing at 1 m distance is 4.5 mR/hr. The radiation protection survey measurements confirm the integrity of radiation safety of the installation, as all the values are within the acceptable limits of 10 μSv hours for the area occupied by the radiation worker and for the general public, respectively.

All examination procedures must be optimized for both image quality and radiation dose, and both must undergo routine quality assurance assessment.[21] The goal of this research was to assess several CT machines. Our findings show that Piranha dosimetry is consistent over time and that there is only minimal acceptable variation in the results of four CT scans, making Piranha a useful tool for quality assurance.

The use of HU measurements for diagnostic purposes is discussed in a number of studies, along with recommendations for tissue features, tissue differentiation, and threshold values for malignant and benign masses, such as in the adrenal glands. The measurements of HU for various item densities between various CT scanners, as well as over time for the same scanner, demonstrate a significant difference in our results.

Radiologists should be aware of this as it pertains to the use of HU for tissue. We suggest that HU may be used cautiously for diagnostic reasons based on the findings of our investigation. The HU is crucial for simulation CT, and the radiation oncologist should beware of lead marker or attenuation factor-induced bone marker artifact.[22] As a result, the artifact will have an impact on treatment planning. To solve this issue, the lead marker should be kept close to the patient, and the marker size should be minimal.

Diagnostic CT scanners typically only have a cradle-shaped couch top; the tabletop is cup-shaped to fit the CT scanner gantry's circular hole. A flat tabletop that closely resembles the tabletop geometry of the treatment machine is necessary for scanners used for CT simulation. The flat tabletop can be either an overlay installed on top of the existing table's cradle or an insert that slips into the cradle of the current table. In terms of treatment setup precision, the CT scanner and the therapy device are directly connected by the tabletop. Poor patient position reproducibility on the treatment equipment results from errors in the scanner tabletop geometry. Vertical and longitudinal movement faults can lead to improper marking of the patient's skin in relation to the calculated treatment isocenter. Improper table indexing can also lead to image spatial distortions. Our investigation found that the patient dose and image quality were unaffected by the CT table's flat or curved surfaces. Scanning techniques were as similar as possible for all scanners. The same Piranha device was, as much as possible, used for measurements on the same CT scanners over time, although different dosimetry was applied for measurements on other CT scanners. However, according to the worldwide organization for radiation safety, there are no discrepancies between four centers using the same dosimetry.

The artifact absorbed in our CT equipment is technically advanced and has to be further improved. To avoid image artifacts, QA adherence has to be followed.[23] Following the occurrence of the streak artifact, beam hardening artifact, ring artifact, and metal artifact due to parameter and technical issues, we conducted a quality control inspection on CT equipment.[24] The result was deemed to be an acceptable limit according to the AERB protocol values.[25]

According to AERB and NABH Quality Assurance for Diagnostic Radiology Machines, two years is sufficient. However, daily QA checks are required for radiotherapy CT machines since CT positioning accuracy and HU units are essential for treatment accuracy.[26]

Conclusion

The result of the mechanical and radiation tests of one CT simulator and three diagnostic CTs shows that Siemens Emotion Duo and GE can be used clinically to obtain optimized images with minimum radiation dose to the patient. It is mandatory to carry out periodic CT QA as per the na-

tional and international CT QA protocols to ensure good quality of image.

Funding

Authors have no funding to report.

Competing interests

The authors have declared that no competing interests exist.

Acknowledgments

The authors have no support to report.

References

1. Nocum DJ, Robinson J, Reed W. The role of quality improvement in radiography. J Med Radiat Sci 2021; 68(3):214–6.
2. Kalra MK, Maher MM, Toth TL, et al. Strategies for CT radiation dose optimization. Radiology 2004; 230(3):619–28. doi: 10.1148/radiol.2303021966
3. Matsubara K, Ichikawa K, Murasaki Y, et al. Accuracy of measuring half-and quarter-value layers and appropriate aperture width of a convenient method using a lead-covered case in X-ray computed tomography. J Appl Clin Med Phys 2014; 15(1):309–16.
4. Kang EJ. Clinical applications of wide-detector CT scanners for cardiothoracic imaging: an update. Korean J Radiol 2019; 20(12):1583.
5. Schmidgunst C, Ritter D, Lang E. Calibration model of a dual gain flat panel detector for 2D and 3D x-ray imaging. Med Phys 2007; 34(9):3649–64.
6. McCollough CH, Leng S, Yu L, et al. CT dose index and patient dose: they are not the same thing. Radiology 2011; 259(2):311–6.
7. Bishnu M, Vijiyan V. In-air calibration of an HDR ^{192}Ir brachytherapy source using therapy ion chambers. J Cancer Res Ther 2005; 1(4):213–20.
8. Descamps C, Gonzalez M, Garrigo E, et al. Measurements of the dose delivered during CT exams using AAPM Task Group Report No. 111. J Appl Clin Med Phys 2012; 13(6):293–302.
9. Rowshanfarzad P, Riis HL, Zimmermann SJ, et al. A comprehensive study of the mechanical performance of gantry, EPID and the MLC assembly in Elekta linacs during gantry rotation. British J Radiol 2015; 88(1051):20140581.
10. DeWerd LA, Micka JA, Laird RW, et al. The effect of spectra on calibration and measurement with mammographic ionization chambers. Med Phys 2002; 29(11):2649–54.
11. Racine D, Viry A, Becce F, et al. Objective comparison of high-contrast spatial resolution and low-contrast detectability for various clinical protocols on multiple CT scanners. Med Phys 2017; 44(9):e153–63.
12. Lin E, Alessio A. What are the basic concepts of temporal, contrast, and spatial resolution in cardiac CT? J Cardiovasc Comput Tomogr 2009; 3(6):403–8.
13. Fitzgerald PF, Colborn RE, Edic PM, et al. CT image contrast of high-Z elements: phantom imaging studies and clinical implications. Radiology 2016; 278(3):723–33.
14. Mkimel M, Mesradi MR, El Baydaoui R, et al. Assessment of computed tomography dose index (CTDI) using the platform GEANT4/GATE. Perspect Sci 2019; 12:100405.
15. Szarmach A, Piskunowicz M, Świętoń D, et al. Radiation safety awareness among medical staff. Polish J Radiol 2015; 80:57.
16. Greffier J, Pereira F, Hamard A, et al. Effect of tin filter-based spectral shaping CT on image quality and radiation dose for routine use on ultralow-dose CT protocols: a phantom study. Diagn Interv Imaging 2020; 101(6):373–81.
17. Hess J, Bender ML, Schilling JG. Evolution of the ratio of strontium-87 to strontium-86 in seawater from Cretaceous to present. Science 1986; 231(4741):979–84.
18. Pang T, Yang B, Liu X, et al. Investigation of absolute dose calibration accuracy for TomoTherapy using real water. J Appl Clin Med Phys 2021; 22(6):139–45.
19. Clausen M, Khachonkham S, Gruber S, et al. Phantom design and dosimetric characterization for multiple simultaneous cell irradiations with active pencil beam scanning. Radiat Environ Biophys 2019; 58:563–73.
20. Saravanakumar A, Vaideki K, Govindarajan KN, et al. Establishment of diagnostic reference levels in computed tomography for select procedures in Pudhuchery, India. J Med Phys 2014; 39(1):50–5.
21. Schumacher A, Sihn W. Development of a monitoring system for implementation of industrial digitalization and automation using 143 key performance indicators. Procedia CIRP 2020; 93:1310–5.
22. Liu Y, Lei Y, Wang Y, et al. Evaluation of a deep learning-based pelvic synthetic CT generation technique for MRI-based prostate proton treatment planning. Phys Med Biol 2019; 64(20):205022.
23. Selles M, Van Osch JA, Maas M, et al. Advances in metal artifact reduction in CT images: A review of traditional and novel metal artifact reduction techniques. Eur J Radiol 2024; 170:111276.
24. Boas FE, Fleischmann D. CT artifacts: causes and reduction techniques. Imaging Med 2012; 4(2):229–40.
25. Tschauner S, Marterer R, Nagy E, et al. Experiences with image quality and radiation dose of cone beam computed tomography (CBCT) and multidetector computed tomography (MDCT) in pediatric extremity trauma. Skeletal Radiology 2020; 49:1939–49.
26. Bannas P, Habermann CR, Jung C, et al. Diagnostic accuracy of state-of-the-art MDCT scanners without gantry tilt in patients with oral and oropharyngeal cancer. Eur J Radiol 2012; 81(12):3947–52.